Available online at www.sciencedirect.com
ScienceDirect
Journal of Molecular Structure 874 (2008) 159–169
Journal of MOLECULAR STRUCTURE
www.elsevier.com/locate/molstruc

An experimental and theoretical study of molecular structure and vibrational spectra of pentafluorophenylboronic acid molecule by density functional theory and ab initio Hartree Fock calculations

Mustafa Kurt

Ahi EvranÜniversitesi Fen edebiyat Fakültesi Fizik Bölümü, Aşıkpaşa Kampusü 40100 Kırşehir-Turkiye, Turkey

Received 10 January 2007; received in revised form 22 March 2007; accepted 23 March 2007
Available online 7 April 2007

Abstract

In this work, the Fourier transform Raman and Fourier transform infrared spectra of pentafluorophenylboronic acid (= pfpba) were recorded in the solid phase. The structural and spectroscopic analysis of the pentafluorophenylboronic acid were made by using ab initio and density functional harmonic and anharmonic calculations. Geometric parameters, Infrared and Raman spectra were compared with single crystal X-ray diffraction data of the molecule. Previous proposed structure for the pfpba derived from the infrared spectra are consistent with the X-ray diffraction data and theoretical calculations.

Keywords: Pentafluorophenylboronic acid (=pfpba); IR and Raman spectra; Density functional theory; Ab initio calculations; Molecular structure

1. Introduction

The boronic acid ligands have been incorporated into various biologically important compounds. A wide variety of boronic acid derivatives of divergent biologically important compounds have been synthesized as anti-metabolites for a possible two-pronged attack on cancer [1–3]. In addition to inhibition of tumor growth, the use of boron-10 neutron capture therapy [4] would be possible owing to the preferential localization of boron compounds in tumor tissue. Boronic acid analogs have been synthesized as transition state analogs for acyl transfer reactions [5] and inhibitors of dihydrotase [6] The boronic acid moiety has also been incorporated into amino acids and nucleosides as anti-tumor, anti-viral agents [7]. Crystal structure of pentafluorophenylboronic acid molecule was investigated by Norton et al.[8]. In order to study these biologically important type of molecules by ab initio Hartree Fock and density functional methods (DFT), the necessary parameters had to be developed.

Up to our knowledge no DFT calculations and detailed vibrational IR and Raman analysis have been performed on pfpba molecule. A detailed quantum chemical study will aid vibrational modes of pfpba and clarifying the experimental data available for this molecule. Density functional theory calculations are reported to provide excellent vibrational frequencies of organic compounds if the calculated frequencies are scaled to compensate for the approximate treatment of electron correlation, for basis set deficiencies and for the anharmonicity [9–14].

Rauhut and Pulay [15] calculated the vibrational spectra of thirty one molecules by using BLYP and B3LYP methods with 6-31G(d) basis set. They reproduced the experimental vibrational frequencies and infrared intensities very well. In their work, they calculated vibrational frequencies of twenty smaller molecules (the training set) whose experimental vibrational frequencies are well assigned, and derived transferable scaling factors by using the least-square method. The scaling factors are successfully applied to other eleven larger molecules (the test set). Even when a single scaling factor of 0.995 (0.963) for the BLYP (B3LYP) method is employed, rms deviations

E-mail address: kurt@gazi.edu.tr

0022-2860/$ - see front matter © 2007 Elsevier B.V. All rights reserved.
doi:10.1016/j.molstruc.2007.03.050

for the training and test sets are 26.2 (18.5) and 26.9 (19.7) cm^{-1}, respectively. Thus vibrational frequencies calculated by using the B3LYP functional with 6-31G(d) basis set can be utilized to eliminate the uncertainties in the fundamental assignments in Infrared and Raman vibrational spectra.

In this work, by using HF and DFT (B3LYP, BLYP) methods, we calculate the vibrational frequencies of pfpba in the ground state to distinguish the fundamentals from the many experimental vibrational frequencies and geometric parameters. These calculations are valuable for providing insight into the vibrational spectrum and molecular parameters.

2. Experimental

The pentafluorophenylboronic acid sample was purchased from Acros Chemical Company with a stated purity of greater than 98% and it was used as such without further purification. The sample pfpba is in solid form at room temperature. Infrared spectra of the sample was recorded between 4000 and 400 cm^{-1} on a Mattson 1000 FTIR spectrometer which was calibrated using polystyrene bands. The sample was prepared as a KBr disc. FT-Raman spectra of the samples were recorded on a Bruker RFS 100/S FT-Raman instrument using 1064 nm excitation from an Nd:YAG laser. The detector is a liquid nitrogen cooled Ge detector. Five hundred scans were accumulated at 4 cm^{-1} resolution using a laser power of 100 mW.

3. Calculations

The geometry data was taken from X-ray structure [8]. The molecular structure of pfpba in the ground state (in vacuo) are optimized by HF, BLYP and B3LYP with the 6-31G(d) and 6-311G(d,p) basis sets. There are no significant difference geometric and vibrational frequencies by the selection of the different basis sets, but we included only geometric parameters for the 6-311g(d,p) basis sets. Three sets of vibrational frequencies for these species are calculated with these methods and then scaled by 0.8929 [16], 0.995 and 0.963, respectively. Molecular geometry is restricted and all the calculations are performed by using Gaussview molecular visualisation program [17] and Gaussian 03 program package on the personal computer [18]. The Becke's three-parameter hybrid density functional, B3LYP [19,20], was used to calculate both harmonic and anharmonic vibrational wavenumbers with the 6-31G* basis set. It is well known in the quantum chemical literature that among available functionals the B3LYP functional yields a good description of harmonic vibrational wavenumbers for small and medium sized molecules.

4. Results and discussion

The molecule of pfpba consists of 16 atoms, so it has 42 normal vibrational modes. On the basis of a C_s symmetry the 42 fundamental vibrations ct form of PFPBA can be distributed as $13A''+28A'$. If we take into account C_{2v} symmetry cc and tt forms of this molecule, 42 normal vibration can be distributed $15A_1+5A_2+8B_1+14B_2$. In the cc, ct and tt forms of molecule, boronic acid and benzene ring are in the same plane. The C_s structure was the lowest in energy at all levels. The molecular structure and numbering of the atoms of pfpba are shown in Fig. 1. We reported some geometric parameters and vibrational frequencies for pfpba by using ab initio Hartree Fock method and DFT(B3LYP and BLYP) comparing some observed bond lengths and bond angles.

5. Geometrical structures

The molecular structure of pfpba has been studied by X-ray diffraction [8]. Total energies and geometry parameters of the molecule are given in Tables 1 and 3, in accordance with the atom numbering scheme given in Fig. 1. The pfba molecule can be all-*trans*, all-*cis* and mixed *trans–cis* relative to the B—C bond. According to theoretical results, the *cis–trans*(ct) conformation is the most stable. Both

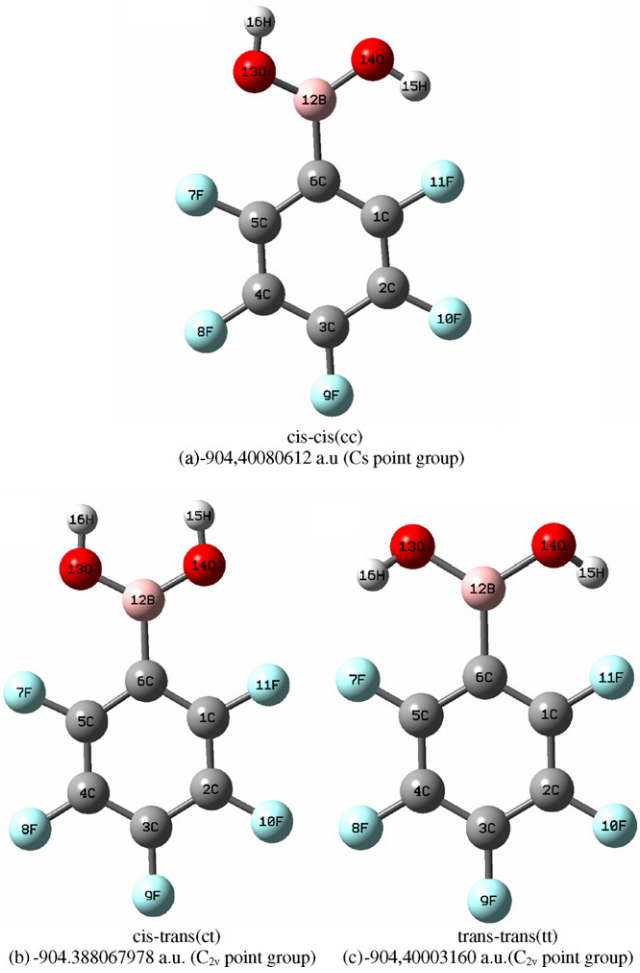

Fig. 1. Structures of pfba and relative conformations of boronic acid group and their energies.

Table 1
Geometric parameter set of pfpba molecule for ct form

	Atom numbering	Exp. [8]	B3LYP(ct)		BLYP(ct)		HF(ct)		B3LYP pentafluorobenzene
			6-31G(d)	6-311G(d,p)	6-31G(d)	6-311G(d,p)	6-31G(d)	6-311G(d,p)	6-31G(d)
Bond lengths									
R1	R(1, 2)	1.384	1.398	1.386	1.400	1.397	1.374	1.372	1.394
R2	R(1, 6)	1.385	1.399	1.396	1.411	1.407	1.388	1.387	1.389
R3	R(1, 11)	1.349	1.359	1.357	1.377	1.377	1.331	1.326	1.34
R4	R(2, 3)	1.372	1.392	1.389	1.404	1.401	1.377	1.376	1.394
R5	R(2, 10)	1.342	1.337	1.336	1.352	1.352	1.317	1.313	1.337
R6	R(3, 4)	1.378	1.391	1.388	1.403	1.399	1.376	1.374	1.394
R7	R(3, 9)	1.334	1.333	1.331	1.349	1.348	1.311	1.306	1.335
R8	R(4, 5)	1.374	1.394	1.391	1.406	1.402	1.379	1.377	1.393
R9	R(4, 8)	1.343	1.337	1.336	1.352	1.352	1.317	1.313	1.337
R10	R(5, 6)	1.374	1.402	1.400	1.414	1.411	1.390	1.389	1.389
R11	R(5, 7)	1.351	1.335	1.334	1.352	1.351	1.313	1.308	1.34
R12	R(6, 12)	1.579	1.586	1.588	1.592	1.594	1.597	1.598	1.083 (C—H)
R13	R(12, 13)	1.355	1.360	1.357	1.365	1.369	1.345	1.342	–
R14	R(12, 14)	1.362	1.365	1.362	1.367	1.375	1.351	1.349	–
R15	R(13, 15)	0.92	0.970	0.963	0.981	0.973	0.948	0.942	–
R16	R(14, 16)	0.82	0.967	0.961	0.978	0.971	0.944	0.939	–
Bond angles									
A1	A(2, 1, 6)	123.0	123.9	123.8	124.1	124.0	123.7	123.6	121.2
A2	A(2, 1, 11)	116.8	115.8	116.0	115.6	115.8	116.2	116.3	118.5
A3	A(6, 1, 11)	120.1	120.1	120.1	120.2	120.1	120.0	120.0	120.2
A4	A(1, 2, 3)	119.2	118.8	118.8	118.7	118.7	118.9	118.9	119.2
A5	A(1, 2, 10)	120.7	120.9	121.0	121.0	121.1	120.8	120.9	120.7
A6	A(3, 2, 10)	120.0	120.1	120.1	120.1	120.1	120.1	120.1	119.9
A7	A(2, 3, 4)	119.7	119.6	119.7	119.6	119.6	119.7	119.8	120.3
A8	A(2, 3, 9)	120.1	120.0	120.0	120.0	120.1	120.0	120.0	119.8
A9	A(4, 3, 9)	120.1	120.2	120.2	120.2	120.2	120.1	120.1	119.8
A10	A(3, 4, 5)	119.4	119.7	119.8	119.7	119.7	119.8	119.8	119.2
A11	A(3, 4, 8)	120.2	119.7	119.6	119.7	119.6	119.7	119.6	119.9
A12	A(5, 4, 8)	120.3	120.5	120.5	120.5	120.6	120.4	120.5	120.7
A13	A(4, 5, 6)	123.0	122.6	122.5	122.8	122.7	122.5	122.4	121.2
A14	A(4, 5, 7)	117.2	116.3	116.2	116.2	116.2	116.3	116.3	118.5
A15	A(6, 5, 7)	119.7	120.9	121.1	120.8	121.1	121.1	121.2	120.2
A16	A(1, 6, 5)	115.3	115.1	115.2	114.8	115.0	115.1	115.3	118.6
A17	A(1, 6, 12)	121.9	121.9	121.9	122.0	122.0	122.1	122.1	120.6 (C—C—H)
A18	A(5, 6, 12)	122.7	122.9	122.7	123.0	122.9	122.7	122.5	120.6
A19	A(6, 12, 13)	118.2	118.7	118.7	118.7	118.8	118.7	118.5	–
A20	A(6, 12, 14)	122.2	122.5	122.9	122.6	123.0	122.8	123.0	–
A21	A(13, 12, 14)	119.5	118.6	118.3	118.5	118.1	118.4	118.3	
A22	A(12, 13, 15)	111.4	109.8	111.0	109.1	110.3	111.7	112.4	–
A23	A(12, 14, 16)	115.6	112.9	114.6	111.7	113.6	116.1	116.9	–

Table 2
Experimental and calculated fundamental harmonic and anharmonic frequencies[a] infrared intensities[b] Raman intensities[c] and energies[d] for ct form

	B3LYP(ct)					BLYP(ct)			HF(ct)			Experimental (in this study)		Approximate assignment[a]
	unscaled	I_{Inf}[b]	I_{Ra}[c]	Scaled[a]	Anharm[a]	unscaled	Scaled[a]	Anharm[a]	unscaled	Scaled[a]	Anharm[a]	IR	Raman	
1	3796	91.36	28.29	3655	3626	3632	3613	3442	4170	3723	3997	3467 m		O—H str.
2	3762	65.97	173.17	3622	3626	3606	3587	3398	4108	3668	3937	3410 m		O—H str.
3	1683	91.26	31.33	1620	1637	1579	1596	1577	1847	1649	1801	1657 m-s	1649 m	C—C str+ ip.C—C—C b+ CCF b.
4	1659	5.39	3.98	1597	1627	1605	1571	1554	1826	1630	1795	1619 sh		C—C—C b.+CCF bend+BCC bend
5	1562	94.23	0.189	1504	1528	1488	1480	1455	1710	1526	1673	1530 s		FCC bend+F—C str
6	1535	608.67	0.644	1478	1502	1465	1457	1426	1677	1497	1644	1490 vs		B—C str, C—C str ,C—F str+B—O str
7	1437	140.41	13.852	1383	1407	1379	1372	1213	1553	1386	1530	1401 m-s	1395 w	C—C str+O—B str+ C—F str+OH—B—C b.
8	1421	46.68	11.12	1368	1389	1357	1350	1326	1519	1356	1491	1377 s		C—C str+O—B str+ C—F str+OH—B—C b.
9	1386	428.59	10.57	1334	1357	1331	1324	1304	1493	1333	1466	1356 m-s		B—C str,B—O—H b.+ F—C str+CCC b.
10	1332	1.04	0,59	1282	1310	1304	1297	1272	1405	1254	1365	1336 m-s		CC str+CCF b.
11	1308	110.46	1,12	1259	1285	1254	1247	1232	1275	1138	1257	1304 m		B—O str+C—F str+BOH b.+CCC b.
12	1170	9.57	1,09	1126	1152	1115	1109	1094	1223	1092	1202	1272 m-s		C—F str+ CCC b. +BOH b.
13	1132	78.67	1.38	1090	1103	1090	1084	1058	1217	1086	1214	1105 s		B—O str+C—F str+BOH b.+CCC b.+
14	1059	218.33	2.31	1019	1014	1040	1034	998	1123	1002	1071	1060 vw		OH—B b.
15	1032	38.69	7.24	993	1000	1002	996	973	1096	978	1067	1028 m		OH—B b.
16	1000	245.95	0.87	963	987	954	949	941	1088	971	1056	977 vs		OHB b.+C—F str+CC str
17	868	41.33	2.36	835	852	836	831	819	926	826	915	926 w		B—C str+B—OH str+C—F str+CCC b.
18	771	1.36	0.24	742	764	741	737	733	839	749	833	862 m		OH——B—C b.+F—C—C b.
19	699	43.59	0.0	673	709	667	663	676	794	708	807	810 m	793 vw	C—B str+B—O str+H—O oop b.
20	639	22.28	1.48	615	629	625	596	612	724	646	744	752 m		H—O oop b.
21	634	0.32	0.26	610	640	599	562	607	707	631	728	708 w		H—O oop b.+oop CCC b.
22	586	5.91	2.09	564	584	565	621	563	670	598	654	670 w	618 vw	Ip OH—B—OH b.+CCC b.+B—C str+CCF b.
23	583	0.07	0.003	561	653	556	553	560	632	564	630	609 w	580 m	Oop CCC b.+B—C str+CCF b. +OH—B—OH b.
24	571	156.91	0.60	549	578	536	533	611	601	536	591	575 w		Oop O—H—B b.
25	556	35.07	16.92	535	553	536	533	532	597	533	575	566 w		Ring breath+OH—B—OH b.+B—C str
26	530	45.35	3.65	510	526	508	505	508	567	506	545	547 vw		Oop O—H—B b.+ Oop CCC b.
27	478	13.25	3.98	460	474	462	459	458	517	461	514	490 vw	490 m	Ip CCC b.+OH—B—OH b.
28	447	0.28	5.08	430	443	432	429	427	485	433	481	431 vw	445 m	Ip CCC b.
29	395	0.41	2.69	380	393	372	370	370	451	402	447			Oop CCC b.+CCF b.
30	359	2.74	1.31	345	355	348	346	342	385	343	387		397 s	Ip OH—B—OH b.+CCF b.
31	350	8.34	0.65	337	343	339	337	332	382	341	383		365 w	Ip O—B—C b.+CCF b.
32	338	2.06	1.26	325	335	322	320	318	375	334	363			Ring wag+B—OH wag
33	312	0.21	0.56	300	308	304	302	299	334	298	330			Ip O—B—C b.+CCF b.
34	298	4.33	1.49	286	296	289	287	287	318	283	306			Ip O—B—C b.+CCF b.
35	277	0.26	0.57	266	276	268	266	269	304	271	303			Ip CCF b.+CCC b.
36	265	0.11	0.10	255	265	256	254	255	294	262	293			Ip CCF b.
37	212	1.99	0.04	204	208	202	200	198	236	210	231			Oop CCF+CCC b.
38	171	1.57	0.11	164	170	167	166	164	181	161	176			ip.B(OH)2 b.
39	129	0.0	0.0	156	159	156	155	152	180	160	176			F—C—C—F twist
40	163	0.04	0.0	124	127	123	122	121	144	128	142			F—C—C—F twist
41	75	0.03	0.07	72	77	73	72	73	82	73	82			Ring+OHBC group wag.
42	29	0.89	0.13	27	52	30	29	49	15	13	7		83 vs	OBCC torsion
E[d]	−904.400806					−904.248917			−900.039504					

[a] Anharm: anharmonic, m: middle, s: strong, vs: very strong, w: weak, vw: very weak, str: stretching, ip: in plane, b.: bending, oop: out-of-plane, wag.: wagging, breath: breathing, twist: twisting.
[b] Infrared Intensities.
[c] Raman intensities.
[d] Energies.

hydrogens are in the O—B—O plane. Most probably, the oxygen lone pairs have a resonance interaction with the empty p orbital of boron, which forces the hydrogen to be in the O—B—O plane. Thus, in the lowest-energy form of pfpba, the $-B(OH)_2$ group is planar and at the whole of computational levels, lies in the plane of the benzene ring. The calculated B—O and B—C bond lengths in pfpba molecule are in good agreement with those found in the X-ray structure [8]. Carbon—fluorine bonds are stronger than carbon—hydrogen bonds. The similar treatment are valid between the C—C ring bond lengths for phenylboronic [7] acid and pfpba molecules by using HF/6-31G(d) level of theory. For example, in the phenylboronic acid (=pfpba) molecule, ring C—C bond lengths varies from 1.386 to 1.394 range, in pfpba molecule these bond lengths varies from 1.376 to 1.388 range. In general, typical B—O distances are 1.359 Å [8] consistent with relatively strong π-interactions. Conversely, the $C_6—B_{12}$ bond length is sligthly greater than that typically found in boroxines, indicating a weakening of this bond by the electron-withdrawing nature of the C_6F_5 group. But by using HF/6-31G(d) levels of theory, for the few boronic acids including phenylboronic acid molecule, Chen et al. found approximately same value of this bond length in Ref. [7].

Bond angles at B and C are consistent sp^2 hybridization but with significant deviations from the expected 120° angles occuring in close proximity the $-B(OH)_2$ substituent on C_6. Thus the experimental values of $C_1—C_6—C_5$, $C_5—C_6—F_7$ and $C_2—C_1—F_{11}$ angles are significantly smaller than the other C—C—C and C—C—F angles respectively. Theoretical calculations are supported by these experimental results (see Table 1).

As can be seen in Table 1, there is good agreement the bond angles at B and C_6. In the pentafluorobenzene molecule, while $C_5—C_6—B$ bond angle is 120.6°, by the boronic acid substitution, this bond angle varies from 122.6° to 122.9°. There are excellent agreements between calculated and experimental bond angles by using HF, BLYP and B3LYP levels of theory. It is interesting that, there are no significant difference of $C_1—C_6—F_{11}$ bond angle between ct and cc form of pfpba molecule. This means that $C_1—C_6—F_{11}$ and $C_5—C_5—F_7$ bond angles are not affected different orientation of H atoms, excluding tt form of pfpba molecule. The experimental results show that, the $-B(OH)_2$ group is twisted by 38.14° relative to the C_6F_5 group. The corresponding calculated value is different from this value (= 0°), because both of C_6F_5 and $B(OH)_2$ groups lie in the same plane. Potential energy scan with the whole levels of theoretical approximation were performed along C—C—B—O torsional angle of pfpba molecule in order to localize the structures that correspond to the energy minima. All the geometrical parameters were simultaneously relaxed during the calculations while the C—C—B—O torsional angle was varied in steps of 10°. The resulted potential energy curve depicted in Fig. 2 shows ct form for minimum energies (Fig. 3).

6. Vibrational spectra

Calculations were made for a free molecule in vacuum, while experiments were performed for solid samples, so there are disagreements between calculated and observed vibrational wavenumbers. According to the theoretical calculation, pfpba has assumed to posses a planar structure of C_s point group symmetry. The 42 normal vibrations are distributed as $13A''+28A'$ considering C_s symmetry. All the 42 fundamental vibrations are active in both IR and Raman. Tables 2 and 4 present the calculated vibrational frequencies and experimental values for ct and cc forms. A comparison of Tables 2 and 4 shows that the vibrational frequencies of the cc conformer lie very close to those of the tc conformer and their assignments are also mostly unchanged Table 4.

The C_s structure was the lowest in energy at all levels. Therefore we ignored the cc and tt conformations (both of them belong to C_{2v} symmetry) of the molecule. All of the calculated modes are numbered from the largest to the smallest frequency within each fundamental wave numbers, $\bar{\nu}$. On the basis on our calculations, and experimental infrared and Raman spectra, we made a reliable one-to-one correspondence between our fundamentals and any of our frequencies calculated by the HF, DFT (B3LYP and BLYP) methods.

Owing to lack of enough detailed experimental data for pfpba molecule, the vibrational spectra was obtained by molecular orbital calculation using Gaussian 03. Vibrational modes of pfpba were investigated by harmonic and

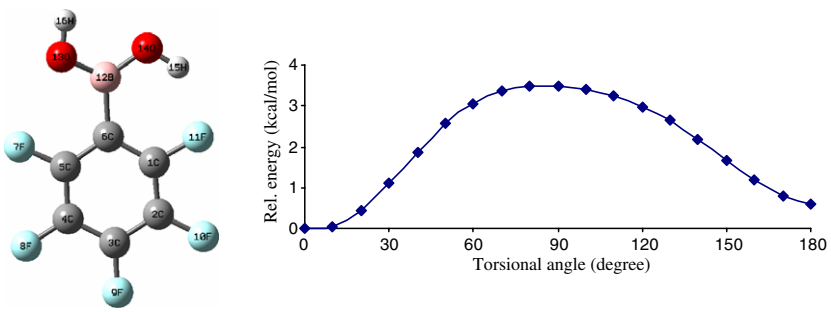

Fig. 2. Torsion profile of C—C—B—O in pentafluorophenylboronic acid by B3LYP/6-31G(d) for ct form.

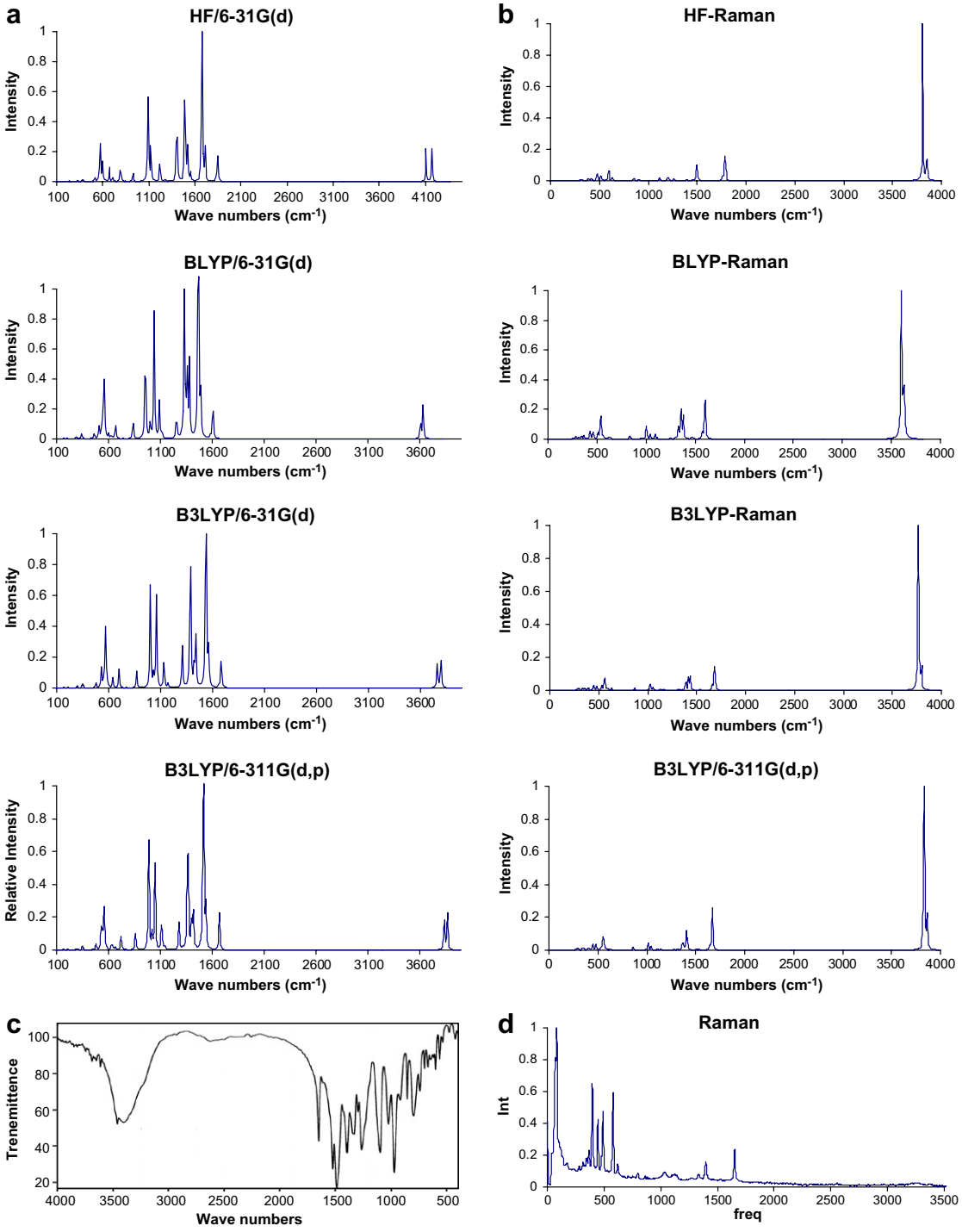

Fig. 3. Comparison of connected frequencies in cm^{-1} and normalized intensities at each level of calculations considered for ct form. (a) Calculated IR spectrum, (b) calculated Raman spectrum of all levels of theory, (c) experimental IR spectrum, (d) experimental Raman spectrum.

in some cases anharmonic frequency calculations performed at the corresponding energy optimised geometries.

The assignment of the vibrational absorptions was made by the comparison with the related molecules and also with the results obtained from the theoretical calculations [21]. The descriptions of the modes presented here are only approximate, being some of the vibration mixed together. Finally, anharmonic vibrational frequencies of pfpba were also calculated explicitly at the HF, BLYP and B3LYP/6-31G(d) levels. The computed fundamental anharmonic frequencies are also reported in Table 2.

As seen in Table 2, two peaks observed for the pfpba in the 2900–3500 cm^{-1} range experimentally in the high frequency region which are 3467 and 3410 m. Otherwise, there are no any peaks at the Raman spectrum in these region. The IR spectra of phenylboronic acid contains

Table 3
Geometric parameter set of pfpba molecule for cc form

	Atom numbering	Exp. [8]	B3LYP(cc)		BLYP(cc)		HF(cc)		B3LYP pentafluorobenzene
			6-31g(d)	6-311G(d,p)	6-31g(d)	6-311g(d,p)	6-31g(d)	6-311G(d,p)	6-31G(d)
Bond lengths									
R1	R(1,2)	1.384	1.388	1.391	1.402	1.402	1.376	1.375	1.394
R2	R(1,6)	1.385	1.397	1.399	1.411	1.411	1.388	1.387	1.389
R3	R(1,11)	1.349	1.354	1.356	1.374	1.374	1.329	1.324	1.34
R4	R(2,3)	1.372	1.390	1.393	1.405	1.405	1.377	1.376	1.394
R5	R(2,10)	1.342	1.334	1.336	1.351	1.351	1.316	1.311	1.337
R6	R(3,4)	1.378	1.390	1.393	1.405	1.405	1.377	1.376	1.394
R7	R(3,9)	1.334	1.331	1.333	1.348	1.348	1.311	1.306	1.335
R8	R(4,5)	1.374	1.388	1.391	1.402	1.402	1.376	1.375	1.393
R9	R(4,8)	1.343	1.334	1.336	1.351	1.351	1.316	1.311	1.337
R10	R(5,6)	1.374	1.397	1.399	1.411	1.411	1.388	1.387	1.389
R11	R(5,7)	1.351	1.354	1.356	1.374	1.374	1.329	1.324	1.34
R12	R(6,12)	1.579	1.604	1.603	1.610	1.610	1.614	1.615	1.083(C—H)
R13	R(7,16)	1.355	1.971	1.944	1.949	1.955	2.004	1.342	–
R14	R(11,15)	1.362	1.971	1.944	1.949	1.955	2.004	1.342	–
R15	R(12,13)	0.92	1.356	1.359	1.371	1.371	1.345	0.938	–
R16	R(12,14)	0.82	1.356	1.359	1.371	1.371	1.345	0.938	–
R17	R(13,16)		0.960	0.966	0.977	0.974	0.944	0.938	
R18	R(14,15)		0.960	0.966	0.977	0.974	0.944	0.938	121.2
Bond angles									118.5
A1	A(2,1,6)	123.0	123.7	123.7	123.9	123.9	123.5	123.5	120.2
A2	A(2,1,11)	116.8	116.2	115.9	115.7	115.8	116.1	116.2	119.2
A3	A(6,1,11)	120.1	120.2	120.2	120.2	120.2	120.2	120.2	120.7
A4	A(1,2,3)	119.2	119.1	119.1	119.0	119.0	119.2	119.2	119.9
A5	A(1,2,10)	120.7	120.9	120.8	120.9	120.9	120.7	120.7	120.3
A6	A(3,2,10)	120.0	119.9	120.0	120.0	120.0	120.0	119.9	119.8
A7	A(2,3,4)	119.7	119.6	119.6	119.6	119.6	119.6	119.7	119.8
A8	A(2,3,9)	120.1	120.1	120.1	120.2	120.2	120.1	120.1	119.2
A9	A(4,3,9)	120.1	120.1	120.1	120.2	120.2	120.1	120.1	119.9
A10	A(3,4,5)	119.4	119.1	119.1	119.0	119.0	119.2	119.2	120.7
A11	A(3,4,8)	120.2	119.9	120.0	120.0	120.0	120.0	119.9	121.2
A12	A(5,4,8)	120.3	120.9	120.8	120.9	120.9	120.7	120.7	118.5
A13	A(4,5,6)	123.0	123.7	123.7	123.9	123.9	123.5	123.5	120.2
A14	A(4,5,7)	117.2	116.0	115.9	115.7	115.8	116.1	116.2	118.6
A15	A(6,5,7)	119.7	120.2	120.2	120.2	120.2	120.2	120.2	120.6(C—C—H)
A16	A(1,6,5)	115.3	114.6	114.6	114.3	114.4	114.6	114.7	120.6
A17	A(1,6,12)	121.9	122.6	122.6	122.8	122.7	122.6	122.6	–
A18	A(5,6,12)	122.7	122.6	122.6	122.8	122.7	122.6	122.6	–
A19	A(6,12,13)	118.2	121.8	121.6	121.8	121.8	121.6	121.7	
A20	A(6,12,14)	122.2	121.8	121.6	121.8	121.8	121.6	121.7	–
A21	A(13,12,14)	119.l5	116.3	116.7	116.3	116.3	116.7	116.5	–
A22	A(12,13,16)	111.4	114.4	112.8	111.7	112.1	116.2	116.9	
A23	A(12,14,15)	115.6	114.4	112.8	111.7	112.1	116.2	116.9	

broad O—H stretching bands at $\overline{\nu} = 3279$ and $3350\ cm^{-1}$, which transform to one sharp band at $\overline{\nu} = 3467\ cm^{-1}$ and one broad band at $\overline{\nu} = 3410\ cm^{-1}$ on formation of pfpba. With the fluorine substitution OH stretching vibrations shifted to higher wavenumbers region [26]. This means that in the boronic acid part OH vibrations are sensitive due to F coordination. The calculated values of O—H stretching modes are overestimated about $188\ cm^{-1}$ for B3LYP, $146\ cm^{-1}$ for BLYP and $256\ cm^{-1}$ for HF methods. The best reliable values are $3442\ cm^{-1}$ harmonic and $3398\ cm^{-1}$ anharmonic calculation for the BLYP method. In the high frequency region, calculated BLYP values are more reliable than HF and B3LYP values for pfpba.

Empirical assignments of vibrational modes for peaks in the fingerprint region are difficult. In the wavenumber region of 600–1660 cm^{-1}, the spectrum observed in the experiments closely resembles the calculated spectrum, except for differences in details.

The sharp and strong band at $1657\ cm^{-1}$ may come from the absorption due to the stretching vibration of the C—C bond, and bending vibration of the C—C—C in the ring part. In the raman spectra, this band corresponds at $1649\ cm^{-1}$. This band observed at $1649\ cm^{-1}$ (Ir), $1657\ cm^{-1}$ (Ir), 1634(Ir)-1633(Ra), for the pentafluorobenzene, α-bromo-pentafluoro-toluene [22] and C_6F_5I [23] molecules, respectively. With the $B(OH)_2$ coordination this mode is not changing significantly. Therefore the mode at

Table 4
Experimental and calculated fundamental harmonic and anharmonic frequencies[a] infrared intensities[b] Raman intensities[c]

	B3LYP(cc)					BLYP(cc)			HF(cc)			Experimental (in this study)[a]		Approximate assignment[a]
	unscaled	I_{Inf}[b]	I_{Ra}[c]	Scaled[a]	Anharm[a]	unscaled	Scaled[a]	Anharm[a]	unscaled	Scaled[a]	Anharm[a]	IR	Raman	
1	3819	36.18	47.28	3668	3650	3662	3517	3473	4187	3762	4016	3467 m		O—H str
2	3816	139.05	2.36	3665	3648	3659	3513	3471	4184	3759	4014	3410 m		O—H str
3	1684	73.27	30.49	1617	1647	1606	1542	1560	1848	1660	1811	1657 m-s	1649 m	C—C str+ ip.C—C—C b+ CCF b.
4	1660	3.80	2.21	1594	1627	1580	1517	1549	1828	1642	1796	1619 sh		C—C—C b.+CCF bend+BCC bend
5	1562	108.95	0.21	1500	1529	1488	1429	1456	1711	1538	1674	1530 s		FCC bend+F—C str
6	1543	550.94	0.73	1482	1507	1477	1418	1443	1679	1508	1646	1490 vs		B—C str, C—C str ,C—F str+B—O str
7	1446	0.01	2.12	1389	1417	1386	1331	1358	1542	1386	1512	1401 m-s	1395 w	C—C str+O—B str+ C—F str+OH—B—C b.
8	1410	75.02	13.22	1354	1374	1340	1287	1310	1535	1379	1507	1377 s		C—C str+O—B str+ C—F str+OH—B—C b.
9	1360	556.72	20.37	1306	1331	1306	1254	1267	1476	1326	1452	1356 m-s		B—C str,B—O—H b.+ F—C str+CCC b.
10	1333	0.01	0.29	1280	1309	1305	1253	1273	1397	1255	1352	1336 m-s		CC str+CCF b.
11	1309	259.98	5.02	1257	1277	1257	1207	1229	1270	1141	1252	1304 m		B—O str+C—F str+BOH b.+CCC b.
12	1165	40.14	1.26	1119	1146	1111	1067	1093	1222	1098	1209	1272 m-s		C—F str+ CCC b. +BOH b.
13	1132	18.73	1.97	1087	1109	1090	1047	1070	1218	1094	1200	1105 s		B—O str+C—F str+BOH b.+CCC b.+
14	1067	224.00	0.46	1025	969	1046	1005	1046	1121	1007	1114	1060 vw		OH—B b.
15	1036	130.92	6.38	995	983	1010	969	966	1087	977	1023	1028 m		OH—B b.
16	996	212.60	0.17	956	984	949	911	935	1086	976	1073	977 vs		OHB b.+C—F str+CC str
17	864	43.05	3.36	830	850	831	798	818	923	829	912	926 w		B—C str+B—OH str+C—F str+CCC b.
18	770	1.35	0.06	739	762	740	711	732	838	753	826	862 m		OH—B—C b.+F—C—C b.
19	687	64.76	0.11	660	701	655	629	667	784	704	802	810 m	793 vw	C—B str+B—O str+H—O oop b.
20	631	0.00	0.04	606	641	611	587	620	721	648	750	752 m		H—O oop b.
21	618	142.73	0.02	593	621	593	570	603	703	632	725	708 w		H—O oop b.+oop CCC b.
22	588	0.53	0.54	564	585	567	544	566	634	569	632	670 w	618 vw	Ip OH—B—OH b.+CCC b.+B—C str+CCF b.
23	582	1.70	0.01	559	662	545	523	536	628	564	618	609 w	580 m	Oop CCC b.+B—C str+CCF b. +OH—B—OH b.
24	566	0.00	13.96	543	549	536	515	601	612	549	603	575 w		Oop O—H—B b.
25	547	27.63	0.71	526	557	517	497	542	609	547	580	566 w		Ring breath+OH—B—OH b.+B—C str
26	530	0.00	1.79	509	546	517	496	540	538	484	518	547 vw		Oop O—H—B b.+ Oop CCC b.
27	484	0.16	6.53	464	479	467	448	462	522	469	510	490 vw	490 m	Ip CCC b.+OH—B—OH b.
28	448	0.31	4.79	430	444	433	415	429	486	437	482	431 vw	445 m	Ip CCC b.
29	396	0.00	2.46	381	393	373	359	370	452	406	450			Oop CCC b.+CCF b.
30	365	0.40	1.21	350	359	353	339	347	391	351	387		397 s	Ip OH—B—OH b.+CCF b.
31	356	6.27	1.22	342	350	345	332	338	386	347	383		365 w	Ip O—B—C b.+CCF b.
32	340	1.28	2.15	327	338	323	310	321	383	344	377			Ring wag+B—OH wag
33	320	3.92	0.27	307	316	311	299	307	342	307	339			Ip O—B—C b.+CCF b.
34	311	7.82	2.48	299	306	302	290	296	328	295	325			Ip O—B—C b.+CCF b.
35	277	0.76	0.64	266	276	268	258	267	304	273	303			Ip CCF b.+CCC b.
36	266	0.41	0.12	256	267	257	247	258	295	265	294			Ip CCF b.
37	214	5.23	0.00	205	210	204	196	200	238	214	235			Oop CCF+CCC b.
38	186	1.76	0.01	178	182	180	173	178	195	175	187			ip.B(OH)2 b.
39	163	0.83	0.02	156	160	156	150	153	181	162	177			F—C—C—F twist
40	131	0.00	0.00	126	129	125	120	123	146	131	143			F—C—C—F twist
41	76	1.78	0.19	73	79	73	70	74	83	75	82			Ring+OHBC group wag
42	38	0.00	0.25	37	70	39	37	70	33	30	29		83 vs	OBCC torsion

[a] Anharm: anharmonic, m: middle, s: strong, vs: very strong, w: weak, vw: very weak, str: stretching, ip: in plane, b.: bending, oop: out-of-plane, wag.: wagging, breath: breathing, twist: twisting.
[b] Infrared Intensities.
[c] Raman intensities.

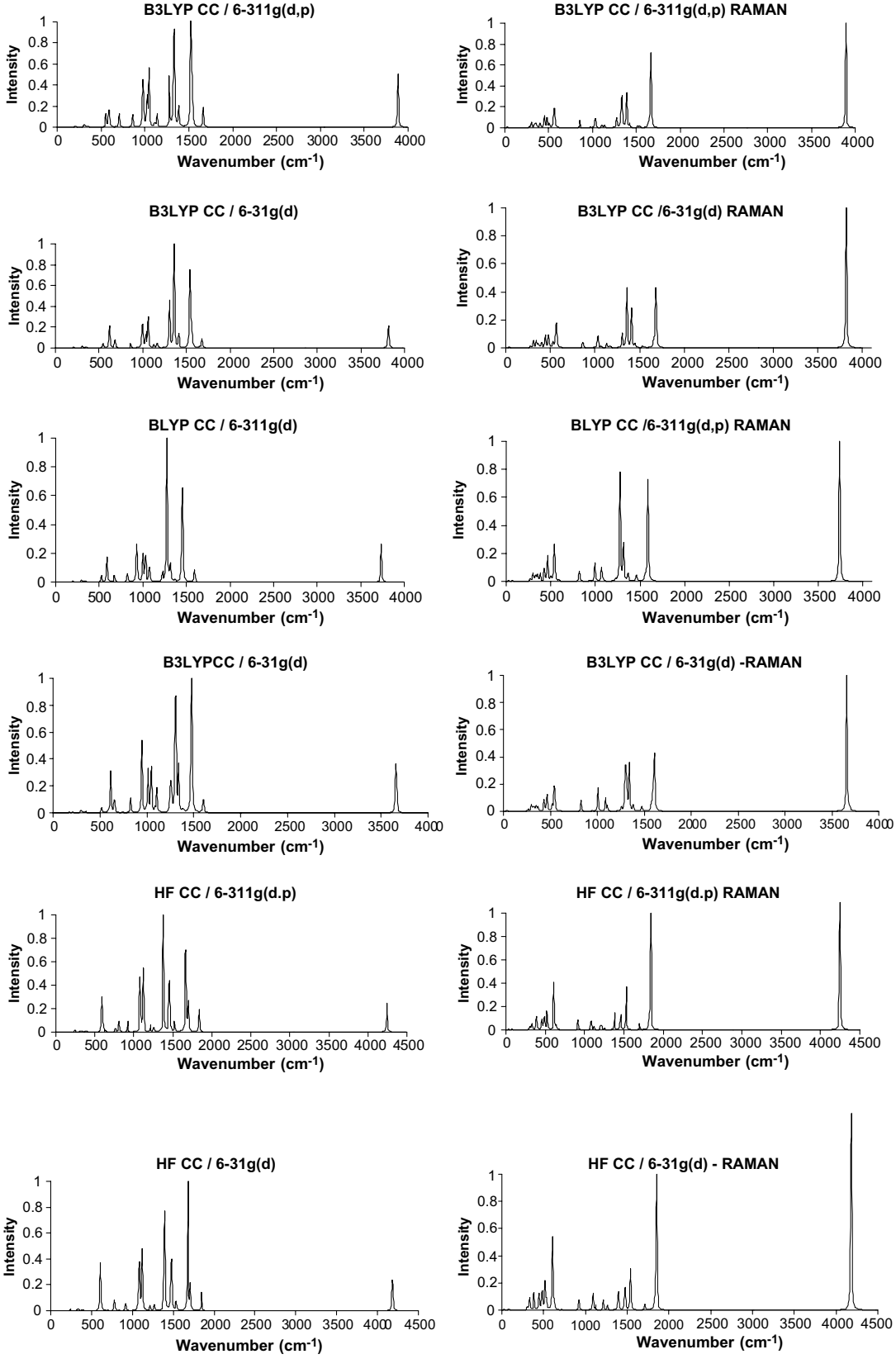

Fig. 4. Comparison of connected IR and Raman frequencies in cm^{-1} and normalized intensities at each level of calculations considered for cc form.

1657 cm^{-1} is insensitive with the $B(OH)_2$ coordination. If we consider phenylboronic acid case, the band at 1607 cm^{-1} shifted to 1657 cm^{-1} [22]. These may be combine effect of fluoro and $B(OH)_2$ substitutions to benzene ring. Best reliable value for this band is 1649 cm^{-1} for HF method contrary to other methods.

Similar comparative analysis has been made for the other selected strong or medium bands. For example; the band at $\overline{v}$ =1377 cm^{-1} is very intense and should include also the υ(B—O) stretching vibration, which for phenylboronic acid is located at $\overline{v}$ =1349 cm^{-1}. Gabriella et al. assigned the band around 1700 cm^{-1} as the υ(B—O) stretching vibrations for the homo- and heterotrinuclear boron complexes [24]. The mode at 1401 cm^{-1} is probably due to a mixture of several motions including C—C and B—O stretching, while the band centered at 1336 cm^{-1} is likely due to vibrational modes involving B—O stretching motions.

In the fluorine compounds, very intense absorption occurs over the 1400–1000 cm^{-1} range. The C—F stretching is observed in the region 1100–1350 cm^{-1} [26,27]. Similarly, the strong band at 1101 cm^{-1} is probably due to C—F stretching and phenyl ring deformation modes. In previous study [25] the bands at 1004, 1001 and 996 cm^{-1} were assigned as a C—F stretching vibrations for some pentafluoro-compounds and pentafluoro-benzyl-bromide [23] molecule. The C—F in-plane bending frequency appears in the region 700–850 cm^{-1}. Sundaraganesan et al. [28] observed strong band at 759 cm^{-1} in FT-IR and very strong band at 750 cm^{-1} in FT-Raman was assigned to C—F in-plane bending mode for 2-amino-4,5-difluorobenzoic acid molecule. In this region except weak modes, we couldnot observe strong or medium absorption band in the experimental FT-IR and FT-Raman spectrum. For the C—F out-of-plane bending mode has been identified as the ~590 cm^{-1}. But our corresponding calculated values did not support from the experimental assignment proposed by Joshi [28] for fluorotoluene and 2-amino-4,5-difluorobenzoic acid molecules (Fig. 4).

The raw boronic acid, C—C and C—F sensitive modes characterized at B3LYP/6-31G(d) level in pfpba molecule are plotted in Fig. 5. The vibrational motions are represented the vector corresponding to the atomic displacement for each atom and computed wavenumbers. Displacement are indicated by dark arrow. The boronic acid, C—C and C—F sensitive modes appear characterized by the direction of the displacement vector. Noted that IR intensities of these modes are medium comparing with the other calculated wavenumbers. As seen in Fig. 5, calculated modes mixed with, C—F, benzene C—C and boronic acid group modes in different proportions.

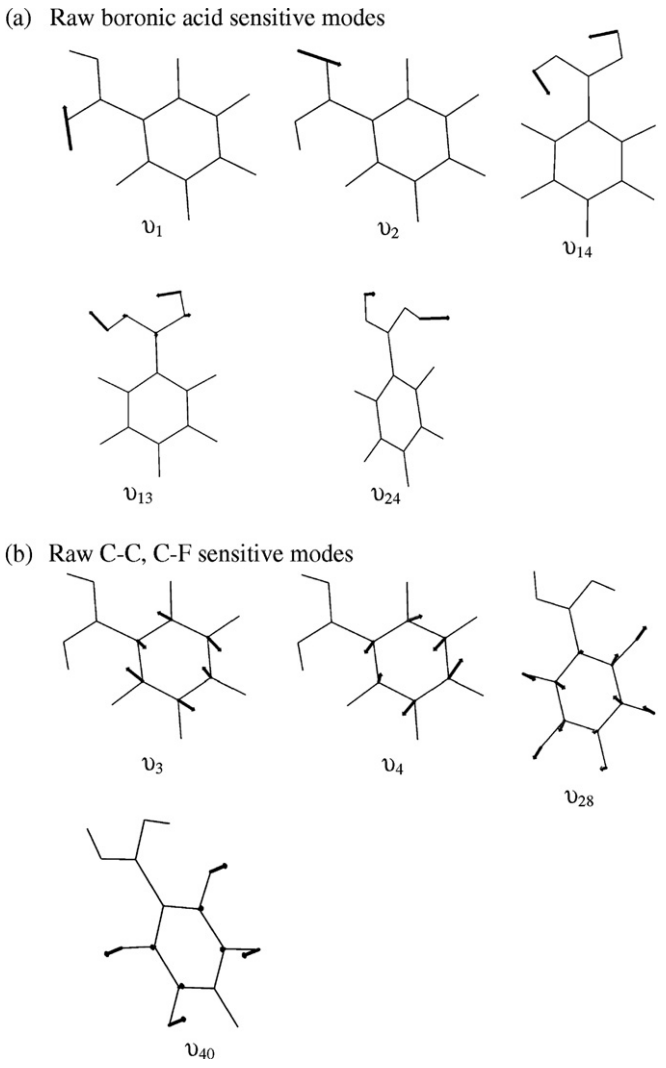

Fig. 5. Raw (a) boronic acid and (b) C—C, C—F sensitive vibrational modes for ct form of studied molecule.

7. Conclusion

Attempts have been made in the present work for the molecular parameters and frequency assignments for the compound pfpba from the FTIR and FT-Raman spectra. The equilibrium geometries, harmonic and anharmonic frequencies of pfpba were determined and analyzed both at HF and DFT level of theories utilizing 6-31G(d) basis sets. The difference between the observed and scaled wave number values of most of the fundamentals is very small. Any discrepancy noted between the observed and the calculated frequencies may be due to the fact that the calculations have been actually done on single molecule in the gaseous state contrary to the experimental values recorded in the presence of intermolecular interactions. Therefore, the assignments made at DFT levels of theory with only reasonable deviations from the experimental values seem to be correct.

Acknowledgements

The Financial support by Gazi University Scientific Research Projects Unit(BAP, Project No: 30-2005/3) is also politely acknowledged. We also thank Professor Dr. Mehmet Somer for Raman measurements in Koç University, Istanbul, Turkey.

References

[1] W. Tjarks, A.K.M. Anisuzzaman, L. Liu, S.H. Soloway, R.F. Barth, D.J. Perkins, D.M. Adams, J. Med. Chem. 35 (1992) 11633–16228.
[2] Y. Yamamoto, Pure Appl. Chem. 63 (1991) 423–426.
[3] F. Alam, A.H. Soloway, R.F. Barth, N. Mafune, D.M. Adam, W.H. Knoth, J. Med. Chem. 32 (1989) 2326–2330.
[4] A.H. Soloway, R.G. Fairchild, Sci. Am. 262 (1990) 100–107.
[5] D.A. Matthews, R.A. Alden, J.J. Birktoft, S.T. Freer, J. Kraut, J. Biol. Chem. 250 (1975) 7120–7126.
[6] D.H. Kinder, S.K. Frank, M.M. Ames, J. Med. Chem. 33 (1990) 819–823.
[7] X. Chen, G. Liang, D. Whitmire, J.P. Bowen, J. Phys.Org. Chem. 11 (1988) 378–386.
[8] P.N. Horton, M.B. Hursthouse, M.A. Becket, M.P.R. Hankey, Acta Cryst. Sect. E Structur Rep. E60 (2004) o2204–o2206.
[9] N.C. Handy, C.W. Murray, R.D. Amos, J. Phys. Chem. 97 (1993) 4392.
[10] P.J. Stephens, F.J. Devlin, C.F. Chavalowski, M.J. Frisch, J. Phys. Chem. 98 (1994) 11623.
[11] F.J. Devlin, J.W. Finley, P.J. Stephens, M.J. Frish, J. Phys. Chem. 99 (1995) 16883.
[12] S.Y. Lee, B.H. Boo, Bull. Korean Chem. Soc. 17 (1996) 754.
[13] S.Y. Lee, B.H. Boo, Bull. Korean Chem. Soc. 17 (1996) 760.
[14] G. Rauhut, P. Pulay, J. Phys. Chem. 99 (1995) 3093.
[15] M.J. Frisch et al., Gaussian 03, Revision B.4, Gaussian Inc., Pittsburgh PA, 2003.
[16] S.H. Vosko, L. Wilk, M. Nusair, Can. J. Phys. 58 (1980) 1200.
[17] P.L. Fast, J. Corchado, M.L. Sanches, D.G. Truhlar, J. Phys. Chem. A 103 (1999) 3139.
[18] A. Frisch, A.B. Nielsen, A.J. Holder, Gaussview Users Manual, Gaussian Inc. Pittsburg.
[19] A.D. Becke, J. Chem. Phys. 98 (1993) 5648.
[20] C. Lee, W. Yang, R.G. Parr, Phys. Rev. B 37 (1988) 785.
[21] Scot H. Brewer, A.M. Allen, S.E. Lappi, T.L. Chase, K.A. Briggman, C.B. Gorman, S. Franzen, Langmuir 20 (2004) 5512–5520.
[22] www.acros.be.
[23] Karsten Koppe, PhD. Thesis, Duisburg University, 2005.
[24] G. Vargas, I. Hernandez, H. Höpfl, M. Ochoa, D. Castillo, N. Farfan, R. Santillan, E. Gomez, Inorg. Chem. 43 (26) (2004) 8490–8500.
[25] A. Papagni, S. Mairona, P.D. Buttero, D. Perdiccia, F. Cariati, E. Cariati, W. Marcolli, Eur. J. Org. Chem. (2002) 1380–1384.
[26] L.J. Bellamy, The Infrared Spectra of Complex molecules, Wiley, New York, 1959.
[27] C.N.R. Rao, Chemical Applications of Infrared Spectroscopy, Academic, Pres, New York, 1959.
[28] N. Sundaraganesan, S. Ilakiamani, B. Dominic Joshua, Spectrochimica Acta Part A 67 (2) (2007) 287–297.